Journal of Materials Chemistry C

Accepted Manuscript

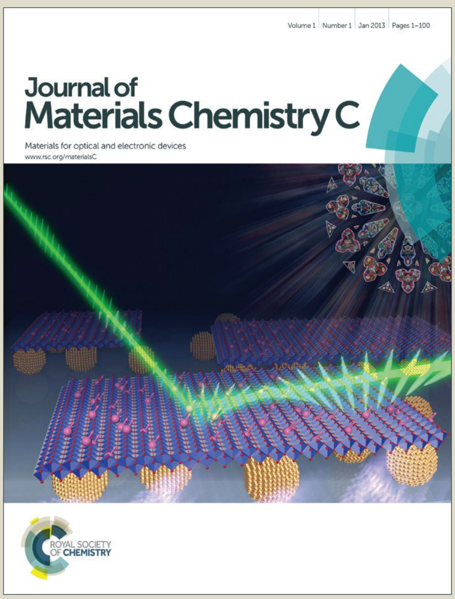

Journal Name

ARTICLE

Chemical Vapour Deposition of Rhenium Disulfide and Rhenium-Doped Molybdenum Disulfide Thin Films Using Single-Source Precursors

Naktal Al-Dulaimi,[a] David J. Lewis,[a,b] Xiang Li Zhong,[b] M. Azad Malik[b] and Paul O'Brien.*[a,b]

Abstract

Polycrystalline thin films of the alloy $Mo_{1-x}Re_xS_2$ ($0 \leq x \leq 0.06$) have been deposited by aerosol-assisted chemical vapour deposition (AA-CVD) using $[Re(\mu\text{-}S^iPr)_3(S^iPr)_6]$ (1) and $[Mo(S_2CNEt_2)_4]$ (2) in different molar ratios at 475 °C. The deposited films were characterised by p-XRD, SEM, ICP-OE, Raman, and EDX spectroscopies. The p-XRD patterns of the films deposited from (1) correspond to ReS_2 and those deposited from (2) matched to MoS_2 (x = 0). Re-doping of up to 6% was achieved in MoS_2 thin films by using different concentrations of precursor (1), the morphology of the doped films changed from lamellar for pure MoS_2 to clusters at 6 mol% alloying with rhenium. The films are promising candidates as models for the incorporation of technetium into transition metal dichalcogenides as a means of immobilisation in nuclear waste processing. Exfoliation of these films is also a potential route towards modification of the optoelectronic properties of 2D molybdenite.

[a] School of Chemistry, The University of Manchester, Oxford Road M13 9PL.

[b] School of Materials, The University of Manchester, Oxford Road, M13 9PL.

Introduction

Two-dimensional transition metal dichalcogenides (TMDCs), which have the general formula MX_2, include molybdenum disulfide (MoS_2), tungsten disulfide (WS_2), and tungsten diselenide (WSe_2) have attracted interest because of their optoelectronic properties in monolayer form[1–3] with useful carrier mobilities and mechanical flexibility.[4–9] MoS_2, in particular, has attracted considerable attention because of its potential applications in hydrogen storage, solid lubricants, capacitors, and electrochemical devices.[10–14] MoS_2 can also be used as a catalyst (e.g. in hydrogen evolution reactions) due to its high-energy crystal edges.[15] The structure of bulk MoS_2 is akin to that of graphite in terms of a repeating layer structure.,[16] held together by non-covalent interactions. $2H$-MoS_2 bulk shows a change from an indirect bandgap to a direct bandgap as the $1H$-MoS_2 monolayer form is approached,[15] as per $MoSe_2$, WSe_2, and WS_2.[17,18] MoS_2 thin films have been synthesised by aerosol assisted chemical vapour deposition (AA-CVD) using metal dithiocarbamate-based precursors. [19] Thin films of MoS_2 doped with Re have been previously synthesised by using spray pyrolysis.[20] We and others have recently developed a general approach to doping MoS_2 with transition metal cations such as chromium based on AA-CVD.[21,22]

Rhenium disulfide (ReS_2) has has a direct bandgap which remains as such in the monolayer form unlike most other TMDCs. Few, if any, changes are observed in the Raman spectrum of monolayer ReS_2 compared to bulk and few-layer variants.[23] Transition metal doped ReS_2 has been reported.[24] Single crystals of Mo-doped $ReSe_2$ have been synthesised by chemical vapour transport method with bromine as a transport agent.[25] The growth of ReS_2 monolayers has been achieved using CVD at 450 °C, the as-deposited ReS_2 is an n-type semiconductor.[26] Colloidal ReS_2 nanoparticles have also been prepared with average size of 5.5 nm.[27] Two-dimensional nanosheets of ReS_2 have been prepared by lithium intercalation, and have unique photocatalytic properties which are superior to other two-dimensional materials.[28] Large area deposition of ReS_2 sheets with good crystallinity has been achieved using simple CVD, from ReO_3 treated with elemental sulfur vapour at 500 °C.[29]

Rhenium-doped MoS_2 can potentially be used as a model for immobilization of radioactive technetium-99 (^{99}Tc).[30] Technetium-99 is very mobile in water; hence there is concern about its release into the environment. In 2008 the production of ^{99}Tc was close to 290 metric tonnes worldwide.[31] Technetium (^{99}T) is produced from uranium fission, and is present in nature at a very low level.[32] The isotope ^{99}Tc has a long half-life (ca. 2×10^5 years), and it forms about 6% of the fission product from uranium.[33,34] The relatively short-lived isotope ^{99m}Tc is a widely used radionuclide in nuclear medicine.[35]

The ionic radii of Tc(IV), Re(IV) and Mo(IV) are 0.65, 0.63 and 0.65 Å respectively, whilst the Shannon-Prewitt crystal radii of Tc(IV), Re(IV) and Mo(IV) are also similar, 0.79, 0.77 and 0.79 Å respectively.[36] The Gibbs free energy change associated with the formation of the M(IV) oxidation state from elemental rhenium and technetium are $\Delta G = 1.3F$ and $1.1F$ kJ mol^{-1} respectively, where F is the Faraday constant.[37] Hence from these data it may be surmised that isovalent substitution of Re into MoS_2 may be performed without significant induced strain in the lattice and minimal free energy penalty from disruption of the host lattice and that rhenium(IV) is a good model for technetium(IV). Entrainment of Re into host structures such as iron phosphate glasses is also known[38]

In this paper we report the deposition of $Mo_{1-x}Re_xS_2$ ($0 \le x \le 0.06$) alloyed thin films using AA-CVD from Mo and Re single source precursors. Molybdenite exists usually as the 2*H* stacked (ABA) polytype ($P6_3mmc$).[39, 40] Rhenium disulfide has a different layered structure that is classified in the $P\bar{1}$ space group,[41] of much lower symmetry than most transition metal dichalcogenides which seems to be driven by the participation of each d^3-Re ion bonding to three others in the same layer which results in the formation of Re_4 parallelograms, with vertices linked in a linear fashion throughout the sheet. The Re-based parallelograms dictate the relative displacements of the sulfur atoms in the hexagonal close packed arrays, and due to this, the sulfur atoms in the layer are rippled on the sheet surface, in contrast to MoS_2, where the sulfur layers appear smooth. At low levels of rhenium incorporation we find that the parent molybdenite structure holds due to the aforementioned similarities in crystal radii and the thermodynamic similarities in their +4 oxidation state. Significantly, this makes Re-doped MoS_2 a potetially useful model system for understanding the thermodynamic stability of ^{99}Tc in a host molybdenum disulfide lattice which will be of particular interest in nuclear chemistry for storage capability-building using inert materials that do not leach radioactive material. This is the first example of single source precursors being used to produce such materials.

Experimental Section

All reactions were carried out under dry nitrogen atmosphere using standard Schlenk techniques. Solvents were purchased from Sigma-Aldrich or Fisher and used without further purification. Reagents were purchased from Sigma-Aldrich.

Instrumentation:

Elemental analysis was performed by the University of Manchester micro-analytical laboratory. A Seiko SSC/S200 model was used for TGA measurements with a heating rate of 10 °C min^{-1} under nitrogen. Scanning electron microscopy (SEM) was performed in secondary electron mode with a Zeiss Ultra55 microscope with an accelerating voltage of 10 kV. Energy-dispersive X-ray (EDX) spectroscopy was performed on the same system at an accelerating voltage of 30 kV using an Oxford Instruments INCA pentaFETx3 detector. A Bruker D8 AXE diffractometer was used to record p-XRD patterns, equipped with a Cu-K_α source (1.5406 Å). Thin films were scanned between 10 and 80° with step size 0.02° and a dwell time of 3 s.

Synthesis of rhenium nonachloride (Re_3Cl_9)

The apparatus was dried by heat gun in a stream of dry nitrogen, and then the apparatus moved with the stopcock closed into a glove bag. Rhenium pentachloride ($ReCl_5$, 2.35 g) was added into the tube and moved from the glove bag and clamped in a vertical way, with a moderate stream of N_2. The tube was heated in a slow Bunsen burner flame, after that the $ReCl_5$ started to melt and the vapour was under reflux. Brown fumes were observed to be liberated. Heating was stopped during the reaction at regular intervals to harvest the crystals which were formed on the wall of tube. This process was repeated until no more brown fumes were liberated and only solid remained.[42] The apparatus was allowed to cool, and the tube sealed off and moved to a nitrogen filled glove bag to transfer the product, black-red solid, into an ampoule. Yield: 72%. Anal. Calc. for Re_3Cl_9 (%): Re, 63.65; Cl, 36.65. Found (%): Re, 61.63; Cl, 36.57.

Synthesis of ($Re_3Cl_9(THF)_3$)

$Re_3Cl_9(THF)_3$ was prepared as previously reported,[43] Re_3Cl_9 (2.3 g, 2.6 mmol) was placed into a thimble in the Soxhlet, then Re_3Cl_9 was extracted from a Soxhlet thimble by refluxing with THF (40 mL) under nitrogen over 48 h or more until the solvent passing through the thimble became colorless. The THF solvent was evacuated and then dark purple solid were collected and washed with diethyl ether (2 x 20 mL). Traces of solvent were removed *in vacuo* to furnish the title product. Yield: 58%. IR (ν_{max} /cm^{-1}): 2956 (w) 1481 (w), 1442 (w), 1336 (w), 1042 (w), 1014(m), 917 (w), 839 (s), 686 (w).

Synthesis of rhenium iso-propylylthiolate $Re_3(\mu\text{-}SPr^i)_3(SPr^i)_6$, (1).

This compound was prepared using the method of Cohen and co-workers.[44] Briefly, $Re_3Cl_9(THF)_3$ (1.7 g, 1.5 mmol) was dissolved in of THF (140 mL). Sodium isopropylthiolate (1.7 g, 17.8 mmol) was added to the red solution of $Re_3Cl_9(THF)_3$. This mixture was refluxed for 48 h after which the THF was removed under reduced pressure. The resulting solid was then extracted by dissolving in hexane five portions of 20 mL; the combined organic phase was filtered through Celite, the solvent was removed by reduced pressure then dried by vacuum oven overnight. Yield: 55%. Anal. calc. for $Re_3S_9C_{27}H_{63}$ (%) C, 26.28; H, 5.14; Found (%) C, 25.82; H, 5.77. ^1H

NMR ($CDCl_3$, 400 MHz,) δ/ppm: 1.18 (d, J=6.81 Hz, 3 H, SCH*Me*$_2$), 1.21 (d, J=6.81 Hz, 3 H, SCH*Me*$_2$) 1.23 (d, J=6.56 Hz, 3 H, SCH*Me*$_2$) 1.27 (d, J=6.81 Hz, 3 H, SCH*Me*$_2$), 1.37 (d, J=6.81 Hz, 4 H, SCH*Me*$_2$), 1.42 (d, J=6.81 Hz, 4 H, SCH*Me*$_2$), 1.58 (d, J=6.81 Hz, 4 H, SCH*Me*$_2$), 1.70 (d, J=4.29 Hz, 3 H, SCH*Me*$_2$), 1.71 (d, J=4.29 Hz, 3 H, SCH*Me*$_2$), 2.84 - 2.96 (septet, 1 H, SCH*Me*$_2$), 3.40 - 3.53 (septet, 1 H, SCH*Me*$_2$), 3.55 - 3.67 (septet, 1 H, SCH*Me*$_2$) , 3.99 - 4.12 (septet, 1 H, SCH*Me*$_2$), 4.19 - 4.32 (septet, 1 H), 4.34 - 4.45 (septet, 1 H, SCH*Me*$_2$), ^{13}C NMR {^1H} ($CDCl_3$, 101 MHz) δ/ ppm: 22.61 (s, 5 C), 25.40 (s, 2 C), 25.71 (s, 2 C), 26.46 (s, 2 C), 27.21 (s, 2 C) 27.78 (s, 2 C), 28.07 (s, 2 C), 28.21 (d, J=2.21 Hz, 5 C), 28.50 (s, 2 C), 30.95 (s, 2 C), 32.23 (s, 1 C), 37.32 (s, 1 C), 37.78 (s, 1 C), 41.46 (s, 2 C), 44.02 (d, J=7.37 Hz, 3 C), 44.05 - 44.28 (m, 2 C), 46.89 (s, 1 C).

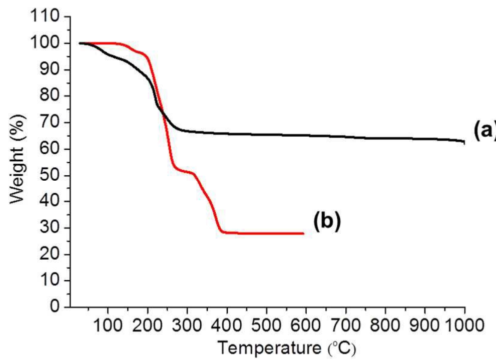

Fig. 1. TGA of (a) Re(μ-S^{i}Pr)$_3$(S^{i}Pr)$_6$ (1) and (b) [Mo(S$_2$CNEt$_2$)$_4$] (2) complexes.

Synthesis of tetrakis(diethylaminodithiocarbomato)molybdate(IV) ([Mo(S$_2$CNEt$_2$)$_4$]), (2).

A mixture of Mo(CO)$_6$ (10g, 37.8 mmol) and *bis*(diethylthiocarbamoyl)disulfide (22.4 g, 75.6 mmol) was dissolved in degassed acetone (400 mL) and heated under reflux at a temperature range of 55-60 °C for 2 h. The mixture was cooled to room temperature, which prompted violet crystals to appear which were filtered and washed with pentane and dried *in vacuo*,[45] to yield the title product as dark microcrystals. Yield: 63 %. Anal Calc. for $C_{20}H_{40}MoN_4S_8$ (%) C, 34.88; H, 5.86; N, 8.14; S, 37.16. Found (%) C, 35.04; H, 6.05; N, 8.08; S37.33. (mp 126-128 °C). MS (ES$^+$) *m/z*: 690.1 [M$^+$H]$^+$.

Aerosol-Assisted Chemical Vapour Deposition (AA-CVD).

AA-CVD was used to deposit the rhenium or molybdenum sulfide thin films by employing [Re(μ-S^{i}Pr)$_3$(S^{i}Pr)$_6$] (1) or[Mo(S$_2$CNEt$_2$)$_4$] (2) , at concentrations of 0.1 mmol in 40 mL of THF at 475 °C. In addition, 0.1 mmol of total precursors (mol [Mo(S$_2$CNEt$_2$)$_4$] and mol [Re(μ-S^{i}Pr)$_3$(S^{i}Pr)$_6$]) were dissolved in (40 mL) THF to give solutions with differing composition (10, 20, 30, and 50 mol%) to synthesis Re-doped MoS_2. Argon was used as inert gas carrier with flow rate 180 sccm in to the furnaces where precursors decomposed and deposit on the glass substrates (1 × 2 cm), which has been ultrasonically cleaned in isopropanol prior to use. The flow rate of argon was controlled using Platon flow gauge. Depositions typically lasted for ca. ~ 3 h

Results and Discussion

Synthesis and Characterisation of the rhenium and molybdenum precursors Re(μ-S^{i}Pr)$_3$(S^{i}Pr)$_6$ (1) and Mo(S$_2$CNEt$_2$)$_4$ (2) were synthesised by literature procedures.[44,45] All characterisation data matched with that previously reported. Complex (1) was a dark red powder, whilst complex (2) appeared as dark purple crystals. Both precursors were freely soluble in THF. Thermogravimetric analysis (TGA) of complexes (1) and (2) was used to determine the thermal decomposition range for both complexes (figure 1). Precursor (1) decomposed in four steps in the temperature ranges of; 40-90 °C, 140-210 °C, and 215-360 °C, followed by a slower decomposition process in the temperature range 810 °C - 1000 °C and complete decomposition occurred after a 10 min. hold at 1000 °C. The remaining mass of residue (62%) suggests the formation of a rhenium sulfide (calc. 61 %) (Figure 1). Precursor **(2)**, had a TGA profile consistent with that previously reported,[22] showing four decomposition steps in the range 0–600 °C with a final residue (29 %) close to that of MoS_2 (calc. 24%).

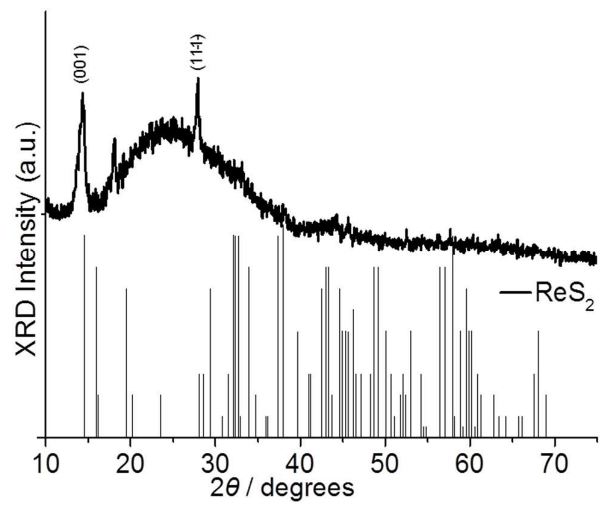

Fig. 2. Powder X-ray diffraction pattern for rhenium disulfide (ReS_2) deposited by AA-CVD using precursor (1) at 475 °C. The black sticks refer to the powder pattern of ReS_2 as reported by Wildervanck et al.[46] A simulated powder pattern is also available in the Supporting Information. The amorphous background is from the glass substrate.

Deposition and Characterization of ReS_2 Thin Films. Deposition of ReS_2 films was performed using AA-CVD. The reactor temperature for deposition of ReS_2, MoS_2, and Re-doped MoS_2 was chosen based on thermogravimetric analysis results (TGA, *vide supra*). Varying molar ratios of precursor (1) and (2) were used in a THF aerosol to achieve doped thin films which were deposited at 475 °C. The films were studied by inductively coupled plasma atomic emission spectroscopy (ICP-AES), powder X-ray diffraction (p-XRD), scanning electron microscopy (SEM) and Raman and energy dispersive X-ray (EDX) spectroscopies. The p-XRD pattern of rhenium disulfide thin films deposited at 475 °C (Figure 2) revealed two major reflections at $2\theta = 14.37°$, which is assigned to the (001) plane of 1T-ReS_2, and at $2\theta = 27.89°$ corresponding to the (111) plane. Thus the ReS_2 produced by AACVD has an apparent preferred orientation in the (001) plane.

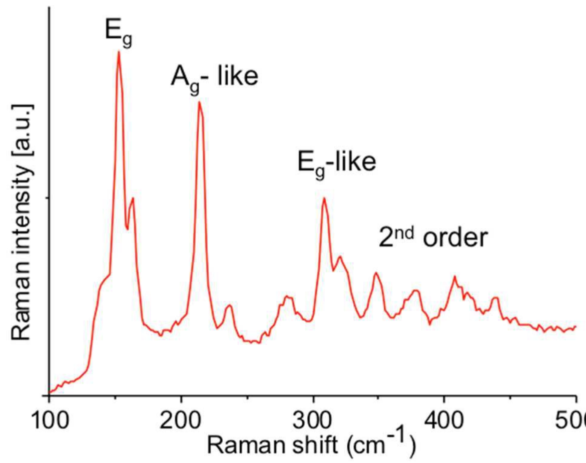

Fig. 3. The Raman spectrum of as-deposited ReS_2 thin films produced by AA-CVD at 475 °C. The profile is consistent with the Raman spectrum of ReS_2 previously reported.[28,29]

Raman spectroscopy of the films revealed three identifiable vibrational modes that can be linked to ReS_2 films. E_g modes, in-plane vibrations of Re atoms in ReS_2, an A_g modes at low frequency, corresponding to the out-of-plane vibrations of Re atoms(Figure 3). The morphological features of thin films of rhenium sulfide were investigated by scanning electron microscopy (SEM), which revealed particles with teardrop morphology (Figure 4a and 4b). Bright field transmission electron microscopy (TEM) reveals that this material is flake-like in appearance at the nanoscale (Figure 4c – 4g), which is consistent with the layered structure of ReS_2. Selected area electron diffraction (SAED) patterns taken from these flakes show that they are highly crystalline (Figure 4h).

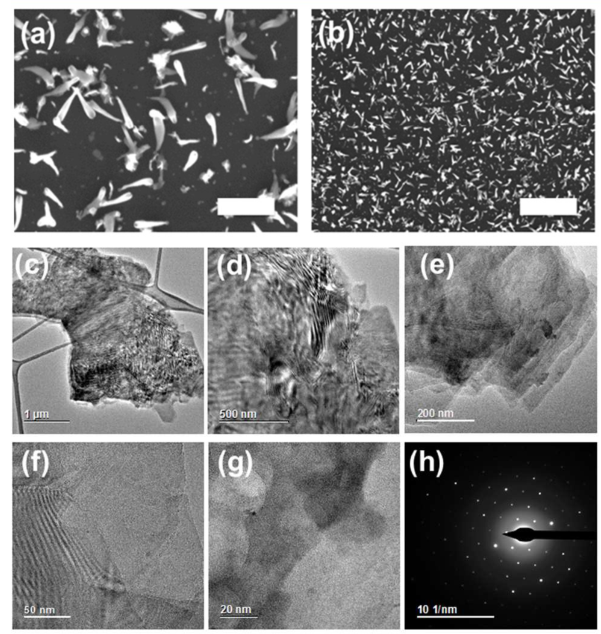

Fig 4. Electron microscopy of rhenium disulfide (ReS_2) thin films. (a) – (b) Secondary electron SEM images (10 kV) of thin films deposited by AA-CVD at 475 °C. Scale bars represent: (a) 2 µm; (b) 5 µm. (c) – (g) Bright field TEM images of ReS_2 thin films (200 kV). (h) Selected area electron diffraction pattern of an ReS_2 flake.

Elemental analysis of the rhenium sulfide thin films by energy dispersive X-ray (EDX) spectroscopy. Thin films of ReS_2 grown from $Re(\mu\text{-}S^iPr)_3(S^iPr)_6$ at 475 °C analysed as follows: Re 30%, S 70% giving a composition of $ReS_{2.3}$. Molybdenum Sulfide was also grown under the same conditions.[19] SEM and EDX and Raman spectroscopies were consistent with that previously reported for this material (Supporting Information).

Deposition and Characterization of Mo-doped ReS_2 Thin Films. Rhenium-alloyed thin films of molybdenum disulfide ($Mo_{1-x}Re_xS_2$ where $0 \leq x \leq 0.06$) were synthesised by AA-CVD at 475 °C. EDX spectroscopy and ICP-OES confirmed that the rhenium dopant was successfully entrained into MoS_2 thin films (Figure 5). In all cases, the incorporation of Re into MoS_2 is inefficient and the amount of Re found by EDX and ICP-OES in the films is only *ca* 10% of that available Re in the aerosol feed.

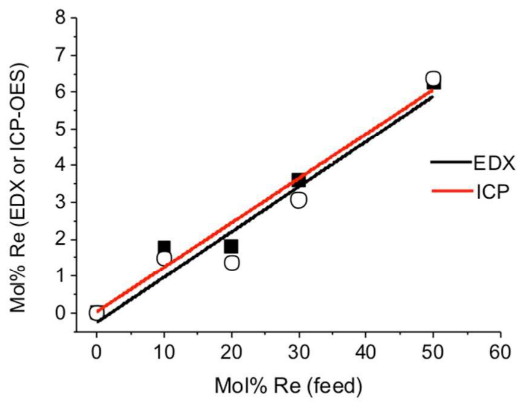

Fig. 5. Plot of mol% Re found in elemental analysis of $Mo_{1-x}Re_xS_2$ ($0 \le x \le 0.06$) thin films produced by AA-CVD at 475 °C by EDX (■) and ICP-OE (○) spectroscopies as a function of varying mol% of Re in the AA-CVD feed.

The p-XRD patterns of $Mo_{1-x}Re_xS_2$ ($0 \le x \le 0.06$) for the ratios 1.79 and 1.80 mol% show four reflections at 2θ = 14.3, 33.2, 39.5, and 58.7° which can be assigned to the (002), (100), (103), and (110) reflections respectively. There was no significant change with the incorporation of 1.79 and 1.80 mol% of Re on the pXRD patterns. However, on increasing the level of Re to more than 1.80 mol%, a significant change in the appearance of the powder patterns was observed. The (002) reflection became weak and broadened (Figure 6). These changes in the powder pattern can be attributed to increasing Re mol%, which affects the stacking layers of the S-Mo-S layers in the basal plane,[47] which has previously been observed for Cr-doped MoS_2 .[21] Bright field TEM of the doped thin films (Supporting Information) reveal that increasing the level of Re in the films does indeed cause a shift to material with a more amorphous appearance. This could potentially be caused the formation of intra-layer Re-Re bonds that locally disrupt the structure by S displacement (*vide supra*). The *d*-spacing for the (002) plane of the MoS_2 film was 6.23 Å which is larger than that reported by Schoenfeld et al.[40] Indeed, in our and other reports of MoS_2 synthesised by AACVD from dithiocarbamato molybdenum(IV) precursors the observed spacings of 6.25 and 6.20 Å,[19,21] suggest that MoS_2 produced by AA-CVD is lattice expanded in the [002] direction as compared to bulk material . The rhenium doped MoS_2 displays a monotonic increase in the *d*-spacing that is linear with doping , suggesting that doping of Re affords a linear lattice expansion in the [002] direction of the crystal. If the literature value of *d*(002) for bulk molybdenite is used,[46] the trend becomes linear. We tentatively suggest that the effect of doping is pseudo-Vegardian.

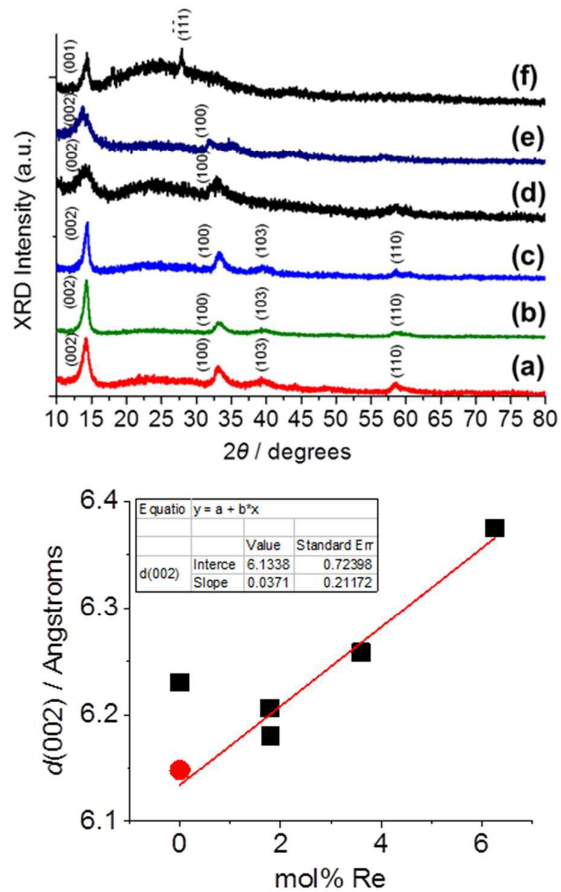

Fig. 6. Powder X-ray diffraction patterns of $Mo_{1-x}Re_xS_2$ ($0 \le x \le 0.06$) films deposited by AA-CVD on glass substrates at 475 °C. Top: full pXRD patterns of (a) 0% Re, (b) 1.79 mol % Re, (c) 1.80 mol % Re, (d) 3.60 mol % Re, (e) 6.25 mol % Re., (f) ReS_2 thin films. Powder patterns are offset for clarity bottom: The *d*(002) spacing for Re- doped MoS_2 measured by pXRD. (●) Literature interlayer distance value of crystalline 2H-MoS_2 (002) 6.15 Å Schoenfeld et al.[40](■) Measured *d*-spacing of MoS_2 and Re-doped MoS_2 from this study. Average value reported by this laboratory for MoS_2 thin films deposited by AA-CVD is 6.23 Å.[19,21] This observation suggests that MoS_2 films produced by AA-CVD generally show lattice expansion in the [002] direction as compared to bulk molybdenite.

Raman spectroscopy was used to study $Mo_{1-x}Re_xS_2$ ($0 \le x \le 0.06$) films. TheMoS_2 film had two main bands observed at 407.6 cm^{-1} and 380.6 cm^{-1} corresponding to the A_{1g} and E_{2g} optical phonon modes (Supporting Information). The Raman spectra for the Re-doped MoS_2 films are shown in Figure 7a. Significant changes in Raman spectra occurred at 3.6 mol% Re with the appearance of a band which could correspond to the A_{1g} mode for ReS_2. Dependence of the Raman shift of the E^1_{2g} and A_{1g} optical modes of $Mo_{1-x}Re_xS_2$ on the amount of Re-dopant is shown in Figure 7b. The difference in the magnitude of the shifts observed for both bands gives insight into the manner of doping.[48] The A_{1g} mode, which consists of the vibrational displacement of sulfur atoms only is only slightly shifted from ca. 407 cm^{-1} to ca. 406 cm^{-1}. On the other hand, the E^1_{2g} mode, which involves the vibration of metal and sulfur atoms in a layer is significantly shifted from ca. 382 cm^{-1} to ca. 376 cm^{-1}. This is consistent with the substitutional doping of the heavier Re atoms into the Mo layer.

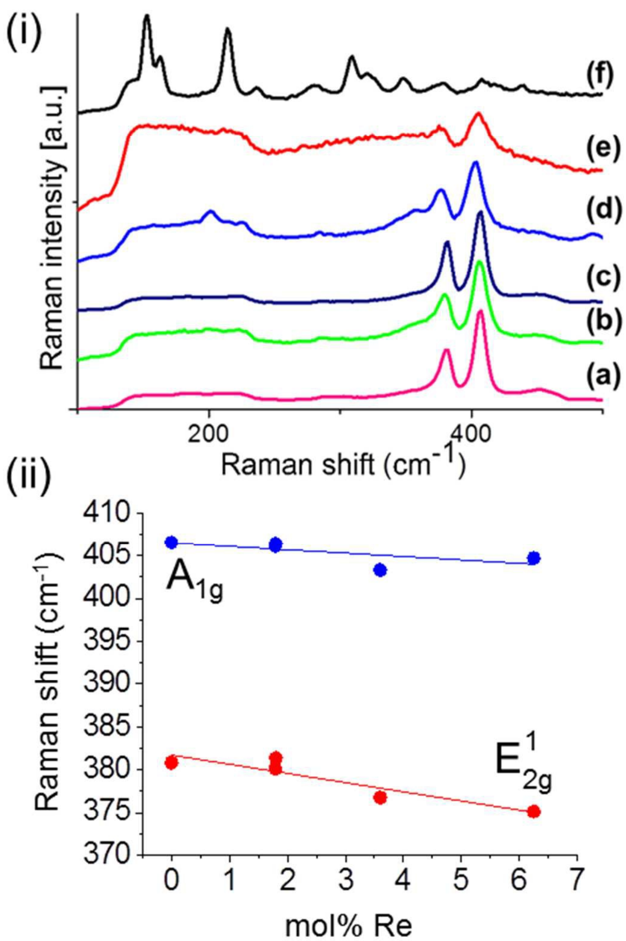

Fig. 7. (i) Raman spectra of $Mo_{1-x}Re_xS_2$ ($0 \le x \le 0.06$) thin films deposited at 475 °C by AA-CVD. (a) MoS2, (b) 1.79 mol % Re, (c) 1.80 mol% Re, (d) 3.60 mol % Re, (e) 6.25 mol% Re, (f) ReS_2. Spectra are stacked for clarity. (ii) Dependence of the Raman shift of the E^1_{2g} and A_{1g} optical modes of $Mo_{1-x}Re_xS_2$ on the amount of Re-dopant.

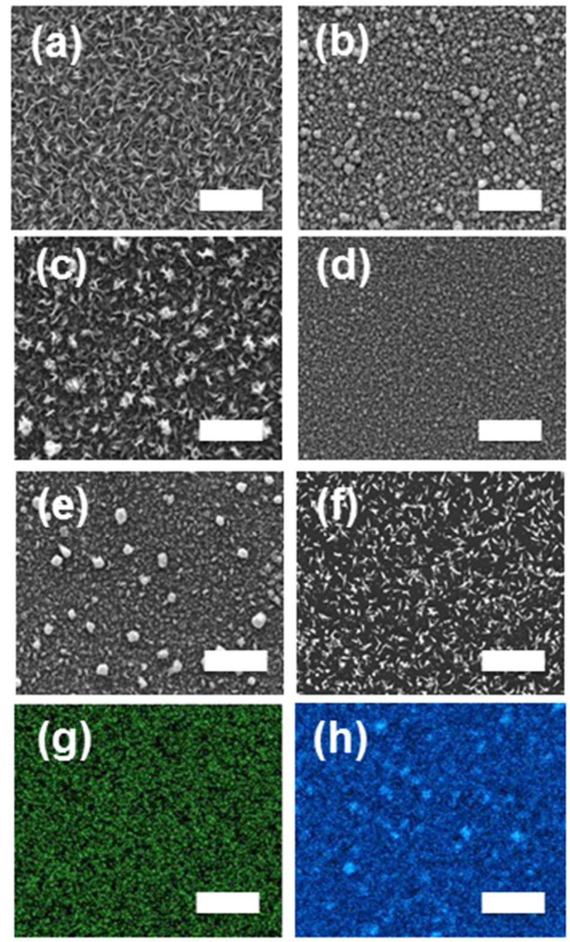

Fig 8. Secondary electron SEM images (10 kV) of $Mo_{1-x}Re_xS_2$ ($0 \le x \le 0.06$) thin films deposited at 475 °C by AA-CVD. (a) 0 mol% Re, (b) 1.79 mol % Re, (c) 1.80 mol % Re, (d) 3.60 mol % Re, (e) 6.25 mol % Re, and (f) ReS_2; thin films were synthesized by using AA-CVD at 475 °C. EDX spectrum maps (30 kV) of (g) Mo L_α and (h) Re K_α emission in 1.8 mol% Re-doped MoS_2 films. All scale bars represent 5 µm.

The surface morphology of the $Mo_{1-x}Re_xS_2$ ($0 \le x \le 0.06$) films deposited by AA-CVD at 475 °C were investigated by SEM. Different morphologies were observed on changing the amount of rhenium; MoS_2 had a lamellar morphology, but Re-doped MoS_2 1.79 % gave clusters. Increasing the Re to 3.60% gave feather-like crystals which were also observed for material with 6.25% Re (Figure 8). Representative elemental mapping of the Re-doped MoS_2 thin film at 1.80% revealed that rhenium is evenly distributed in the film (Figure 8). This was found in all alloyed films, suggesting that the isovalent substitution of Re(IV) for Mo(IV) was homogeneous under the conditions employed in this study.

Conclusions

Thin films of $Mo_{1-x}Re_xS_2$ ($0 \leq x \leq 0.06$) were deposited by AA-CVD from the single-source precursors $Re(\mu\text{-}S^iPr)_3(S^iPr)_6$ (**1**) and $Mo(S_2CNEt_2)_4$ (**2**). The Re-doped MoS_2 thin films were deposited by using different molar ratios of (**1**) and (**2**). The morphology of thin films as investigated by SEM changes as the doping of MoS_2 with rhenium is increased The p-XRD patterns for the Re-doped MoS_2 shows systematic variations in the peak shape, intensity, and the position of the (002) planes as the rhenium content varies. The *d*(002) spacing in the alloys increases in a pseudo-Vegardian manner. EDX mapping of films demonstrated the spatial homogeneity of the doping. The MoS_2 alloy with Re is a promising as a model system for the stability of ^{99}Tc in the host molybdenum disulfide crystal due to crystal radii and thermodynamic similarities between Re(IV) and Tc(IV). The materials could also be exfoliated either by liquid or mechanical means to make novel 2D materials; we are currently investigating this possibility.

Acknowledgements

N Al-D thanks the Higher Committee for Education Development in Iraq (HCED) for funding and support, and also, the Chemistry Department and University of Sulaimani, Iraq, for allowing a period of study in the U.K. Some of the equipment used in this study were provided by the Engineering and Physical Sciences Research Council U. K. (Core Capability in Chemistry, EPSRC grant number EP/K039547/1).

Supporting Information Available: Characterization of MoS_2 thin films produced by AA-CVD at 475 °C, simulated pXRD pattern of ReS_2.

Corresponding Author

* Professor Paul O'Brien CBE FRS. The University of Manchester, Oxford Road, M139PL, Email: Paul.O'Brien@manchester.ac.uk. Tel: +44 (0) 161 275 4652

Notes and references

1 Q. H. Wang, K. Kalantar-Zadeh, A. Kis, J. N. Coleman and M. S. Strano, *Nat Nano*, 2012, **7**, 699–712.

2 M. Chhowalla, H. S. Shin, G. Eda, L.-J. Li, K. P. Loh and H. Zhang, *Nat. Chem.*, 2013, **5**, 263–275.

3 S. Z. Butler, S. M. Hollen, L. Cao, Y. Cui, J. A. Gupta, H. R. Gutiérrez, T. F. Heinz, S. S. Hong, J. Huang, A. F. Ismach, E. Johnston-Halperin, M. Kuno, V. V Plashnitsa, R. D. Robinson, R. S. Ruoff, S. Salahuddin, J. Shan, L. Shi, M. G. Spencer, M. Terrones, W. Windl and J. E. Goldberger, *ACS Nano*, 2013, **7**, 2898–2926.

4 RadisavljevicB., RadenovicA., BrivioJ., GiacomettiV. and KisA., *Nat Nano*, 2011, **6**, 147–150.

5 D. Lembke and A. Kis, *ACS Nano*, 2012, **6**, 10070–10075.

6 D. Jariwala, V. K. Sangwan, L. J. Lauhon, T. J. Marks and M. C. Hersam, *ACS Nano*, 2014, **8**, 1102–1120.

7 H.-Y. Chang, S. Yang, J. Lee, L. Tao, W.-S. Hwang, D. Jena, N. Lu and D. Akinwande, *ACS Nano*, 2013, **7**, 5446–5452.

8 B. W. H. Baugher, H. O. H. Churchill, Y. Yang and P. Jarillo-Herrero, *Nano Lett.*, 2013, **13**, 4212–4216.

9 A. Abderrahmane, P. J. Ko, T. V Thu, S. Ishizawa, T. Takamura and A. Sandhu, *Nanotechnology*, 2014, **25**, 365202.

10 M. Sun, J. Adjaye and A. E. Nelson, *Appl. Catal. A Gen.*, 2004, **263**, 131–143.

11 W. M. R. Divigalpitiya, R. F. Frindt and S. R. Morrison, *Science* 1989, **246**, 369–371.

12 S. Ding, J. S. Chen and X. W. (David) Lou, *Chem. Eur. J.*, 2011, **17**, 13142–13145.

13 M. Chhowalla and G. A. J. Amaratunga, *Nature*, 2000, **407**, 164–167.

14 J. Chen, N. Kuriyama, H. Yuan, H. T. Takeshita and T. Sakai, *J. Am. Chem. Soc.*, 2001, **123**, 11813–11814.

15 K. F. Mak, C. Lee, J. Hone, J. Shan and T. F. Heinz, *Phys. Rev. Lett.*, 2010, **105**, 136805.

16 K. Chang, D. Geng, X. Li, J. Yang, Y. Tang, M. Cai, R. Li and X. Sun, *Adv. Energy Mater.*, 2013, **3**, 839–844.

17 S. Tongay, J. Zhou, C. Ataca, K. Lo, T. S. Matthews, J. Li, J. C. Grossman and J. Wu, *Nano Lett.*, 2012, **12**, 5576–5580.

18 W. Zhao, R. M. Ribeiro, M. Toh, A. Carvalho, C. Kloc, A. H. Castro Neto and G. Eda, *Nano Lett.*, 2013, **13**, 5627–5634.

19 A. Adeogun, M. Afzaal and P. O'Brien, *Chem. Vap. Depos.*, 2006, **12**, 597–599.

20 V. A. Kuznetsov, A. S. Berdinsky, A. Y. Ledneva, S. B. Artemkina, M. S. Tarasenko and V. E. Fedorov, *Sensors Actuators A Phys.*, 2015, **226**, 5–10.

21 (a) D. J. Lewis, A. A. Tedstone, X. L. Zhong, E. A. Lewis, A. Rooney, N. Savjani, J. R. Brent, S. J. Haigh, M. G. Burke, C. A. Muryn, J. M. Raftery, C. Warrens, K. West, S. Gaemers and P. O'Brien, *Chem. Mater.*, 2015, **27**, 1367–1374. (b) A. A. Tedstone, D. J. Lewis, R. Hao, S.-M. Mao, P. Bellon, R. S. Averback, C. P. Warrens, K. R. West, P. Howard, S. Gaemers, S. J. Dillon and P. O'Brien, *ACS Appl. Mater. Interfaces*, 2015, *7*, 20829-20834.

22 M. N. McCain, B. He, J. Sanati, Q. J. Wang and T. J. Marks, *Chem. Mater.*, 2008, **20**, 5438–5443.

23 S. Tongay, H. Sahin, C. Ko, A. Luce, W. Fan, K. Liu, J. Zhou, Y.-S. Huang, C.-H. Ho, J. Yan and others, *Nat. Commun.*, 2014, **5**, 1–6.

24 D. Çakir, H. Sahin and F. M. Peeters, *Phys. Chem. Chem. Phys.*, 2014, **16**, 16771–16779.

25 S. Yang, S. Tongay, Q. Yue, Y. Li, B. Li and F. Lu, *Sci. Rep.*, 2014, **4**, 1–6.

26 K. Keyshar, Y. Gong, G. Ye, G. Brunetto, W. Zhou, D. P. Cole, K. Hackenberg, Y. He, L. Machado, M. Kabbani and others, *Adv. Mater.*, 2015, **27**, 4640–4648.

27 W. Tu and B. Denizot, *J. Colloid Interface Sci.*, 2007, **310**,

167–170.

28 T. Fujita, Y. Ito, Y. Tan, H. Yamaguchi, D. Hojo, A. Hirata, D. Voiry, M. Chhowalla and M. Chen, *Nanoscale*, 2014, **6**, 12458–12462.

29 K. Xu, H.-X. Deng, Z. Wang, Y. Huang, F. Wang, S.-S. Li, J.-W. Luo and J. He, *Nanoscale*, 2015, **7**, 15757–15762.

30 H. Matzke and E. Vernaz, *J. Nucl. Mater.*, 1993, **201**, 295–309.

31 J. P. Icenhower, N. P. Qafoku, J. M. Zachara, D. M. Wellman and W. J. Martin, .

32 B. T. Kenna and P. K. Kuroda, *J. Inorg. Nucl. Chem.*, 1964, **26**, 493–499.

33 K. Morris, F. R. Livens, J. M. Charnock, I. T. Burke, J. M. McBeth, J. D. C. Begg, C. Boothman and J. R. Lloyd, *Appl. Geochemistry*, 2008, **23**, 603–617.

34 V. Neck and B. Kanellakopulos, *Radiochim. Acta*, 1987, **42**, 135–138.

35 B. M. Dantas, A. L. A. Dantas, F. L. N. Marques, L. Bertelli and M. G. Stabin, *Brazilian Arch. Biol. Technol.*, 2005, **48**, 215–220.

36 R. D. t Shannon, *Acta Crystallogr. Sect. A Cryst. Physics, Diffraction, Theor. Gen. Crystallogr.*, 1976, **32**, 751–767.

37 G. E. Boyd and Q. V Larson, *J. Phys. Chem.*, 1956, **60**, 707–715.

38 K. Xu, P. Hrma, W. Um and J. Heo, *J. Nucl. Mater.*, 2013, **441**, 262–266.

39 R. G. Dickinson and L. Pauling, *J. Am. Chem. Soc.*, 1923, **45**, 1466–1471.

40 B. Schönfeld, J. J. Huang and S. C. Moss, *Acta Crystallogr. Sect. B Struct. Sci.*, 1983, **39**, 404–407.

41 H. H. Murray, S. P. Kelty, R. R. Chianelli and C. S. Day, *Inorg. Chem.*, 1994, **33**, 4418–4420.

42 R. Lincoln and G. Wilkinson, *Inorganic synthesis*, 1980, vol. XX.

43 K. Mertis, P. G. Edwards, G. Wilkinson, K. M. A. Malik and M. B. Hursthouse, *J. Chem. Soc. Dalt. Trans.*, 1981, 705–716.

44 W.-W. Zhuang, D. M. Hoffman, D. Lappas and J. Cohen, *Polyhedron*, 1998, **17**, 2583–2586.

45 T. Ouyang, K. P. Loh, H. Zhang, J. J. Vittal, M. Vetrichelvan, W. Chen, X. Gao and A. T. S. Wee, *J. Phys. Chem. B*, 2004, **108**, 17537–17545.

46 J. C. Wildervanck and F. Jellinek, *J. Less Common Met.*, 1971, **24**, 73–81.

47 L. Ye, S. Chen, W. Li, M. Pi, T. Wu and D. Zhang, *J. Phys. Chem. C*, 2015, **119**, 9560–9567.

48 C. Lee, H. Yan, L. E. Brus, T. F. Heinz, J. Hone and S. Ryu, *ACS Nano* 2010, ***4***, 2695-2700.

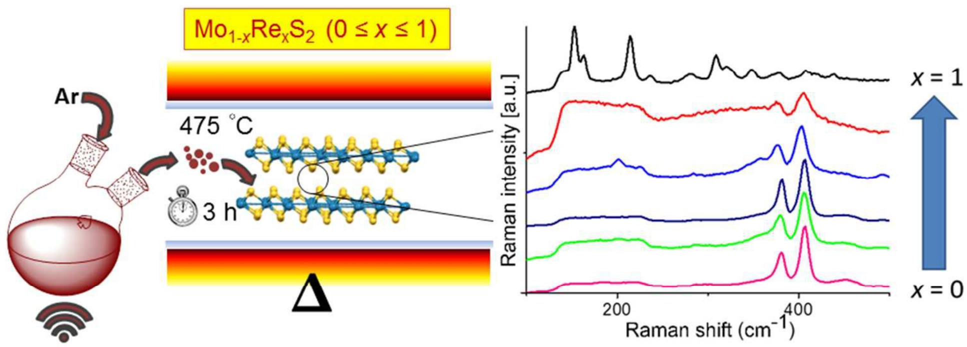

254x190mm (96 x 96 DPI)